Localised corrosion of super duplex stainless steel in synthetic NaOH-Na₂S solution at different temperatures

Corrosión localizada del acero inoxidable súper dúplex en solución sintética de NaOH-Na₂S a diferentes temperaturas

Carlos Rondón-Almeyda [iD][1]*, Lina Sierra-Serrano [iD][1], Mauricio Rincón-Ortiz [iD][1]

[1]Grupo de Investigación en Desarrollo y Tecnología de Nuevos Materiales, Universidad Industrial de Santander UIS. Calle 9 # Carrera 27. C. P. 680002. Bucaramanga, Colombia.

ABSTRACT: The pitting corrosion resistance of the UNS S-32760 super duplex stainless steel (SDSS) in synthetic NaOH-Na₂S solution at different working temperatures of 25, 50, and 70°C has been evaluated in the current investigation to assess the alloy behaviour under the caustic environments used in the pulp and paper industry. The temperature effect on pitting (Ep) and repassivation (Erp) potentials was studied with the Cyclic Potentiodynamic Polarisation (CPP) technique according to the ASTM G61. Results demonstrated that pitting corrosion is prone to occur when increasing alloy temperature since both pitting and repassivation potentials lean towards more negative values while the repassivation zone is reduced. Furthermore, the morphology of the found pits was determined using Scanning Electron Microscopy (SEM). The pitting corrosion mechanism for the studied super duplex stainless steel under the exposed conditions was introduced. The thiosulphate ion is attributed to be responsible for the initiation of the localised corrosion.

RESUMEN: La resistencia a la corrosión por picado del acero inoxidable súper dúplex UNS S-32760 en una solución sintética de NaOH y Na₂S a diferentes temperaturas de trabajo 25°, 50° y 70°C fue estudiada en la presente investigación, con el propósito de evaluar el comportamiento de la aleación en ambientes cáusticos utilizados en la industria de la pulpa y el papel. Se utilizó la técnica electroquímica de Polarización Potenciodinámica Cíclica (PPC) acorde a ASTM G61 para estudiar el efecto de la temperatura en los potenciales de picado (Ep) y repasivación (Erp). Los resultados mostraron, que al incrementar la temperatura la aleación es más susceptible a la corrosión por picado, ya que tanto los potenciales de picado como los potenciales de repasivación tienden a valores más negativos y la zona de repasivación se reduce. Por otro lado, se realizó una caracterización utilizando Microscopia Electrónica de Barrido (SEM) para determinar la morfología de las picaduras encontradas. El mecanismo de corrosión por picado para el acero inoxidable súper dúplex en las condiciones expuestas, se atribuye al ion tiosulfato ser el encargado de iniciar la corrosión localizada.

1. Introduction

The invention and later manufacture of paper were originally created with the intention of documenting and recording acts and bureaucratic agreements. At the very beginning, some challenges faced by the paper industry were the lack of raw materials such as fabrics, cotton, grass, etc., being not sufficient to supply the production demand. However, in the 19th and 20th centuries, distinct chemical mechanisms were developed to obtain cellulose fibres as raw material, increase the production, and position this industry as one of the cultural development promoters [1, 2].

The chemical process based on the usage of caustic soda, sulphites, and sulphates, permits the production of pulp and paper, being the sulphate, or Kraft Pulp technique, the widest method applied at an industrial level [2, 3]. Currently, some efforts have been concentrated

* Corresponding author: Carlos Rondón Almeyda

E-mail: carlos2188233@correo.uis.edu.co

to improve efficiency, cost, and the protection of the environment through the partial recovery of energy and reagents, components associated with the application of materials [3].

The Kraft pulping process starts off with a primary series of reactors known as digesters, where a solution labelled as white liquor, primarily composed of sodium hydroxide (NaOH) and sodium sulphide (Na$_2$S), is added. Sulphide is mainly present, forming hydrated sulphur ions (HS$^-$) in the form of sulphides (S^{2-}) and poly-sulphides. Additionally, sulphur anions as sulphates (SO$_4^{2-}$), sulphites (SO$_3^{2-}$), and thiosulphates (S$_2$O$_3^{2-}$) can also be obtained due to oxidation; hence, white liquor is an aggressive solution that induces corrosion problems for the paper industry [2, 4–6].

Initially, the digestors were fabricated using carbon steels with high wall thicknesses, causing an increase in production costs [3]. Consecutively, these were manufactured with an internal stainless-steel coating, yet poor adhesion was reported, resulting unfavourable for the industry [2, 7]. Over the past few decades, researchers have spotlighted their interest in using different duplex stainless steels, which are characterised by having a biphasic microstructure (ferrite-austenite) to attain better results in terms of investment, production, and maintenance values [7–9].

Particularly, carbon steels (ASTM A516 GR 70 and A285 Type C), employed for the fabrication of Kraft digestors, immersed in white liquor simulated solutions, have shown to be sensitive to stress corrosion cracking [10]. Similarly, the corrosion behaviour of a 316L stainless-steel was studied under caustic environments with a maximum temperature of 90°C, establishing that the steel shows a maximum 18mm/year corrosion rate [11]. The uniform corrosion rate of three stainless steels (UNS S32304, S31803, and S31803) was evaluated by weight loss under conditions that simulated a digester at 170°C, exhibiting that the UNS S32304 steel has better corrosion resistance, attributed mainly to the higher chromium content [12]. Additionally, it was determined that white liquor at a temperature of 88°C seems to be detrimental for carbon steels used in the Kraft process, increasing corrosion kinetics as sulphide ions are added, while stainless steels presented a significant enhancement of the corrosion resistance. This led to conclude that the UNS 31803 duplex stainless-steel improves corrosion problems at the tested temperature because of the presence of almost similar amounts of ferrite and austenite [9]. Besides, it was confirmed that Na$_2$S inhibits the arrangement of a stable passive film, incrementing corrosion in substances containing sulphides [13].

Potentiodynamic polarisation techniques were used to determine that the quantity of sodium sulphide, together with a rise in temperature, increase the corrosion rate of the UNS S32110, UNS S32205, and UNS S32304 super duplex stainless steels (SDSS) [5]. A study reported that UNS S32101, UNS S32205, and UNS S32304 duplex steels, when exposed to a synthetic white liquor solution and temperatures ranging from 90 to 100°C, exhibit a higher resistance due to their remarkably alloyed nature [14]. Likewise, different tests in 31803 and 32304 duplex stainless steels exposed to white liquor solutions were studied by means of Cyclic Potentiodynamic Polarisation (CPP) curves, showing that while increasing temperature, the transpassive potential decreases, making steels vulnerable to corrosion [15]. Finally, it was reported that corrosion augments when increasing temperature, and on this matter, S32750 SDSS has a surpassed behaviour against corrosion in contrast to the S32205 duplex steel [4].

The objective of this work was the localised corrosion study of a UNS S-32760 SDSS over the critical potentials (Erp and Ep), while employing CPP in synthetic Na(OH) at different temperatures.

2. Experimental Methods

2.1 Material

The material used in this study was a UNS S-32760 SDSS rod with a diameter of 11.35 mm, from where the cross and longitudinal sections were taken and mounted on the synthetic resin (Bakelite). The samples were grinded and cloth polished using diamond paste. A metallographic analysis was performed etching the sample with a 10% oxalic acid while administering a 3V potential for 2 min and a 1.5 cm electrode gap. The microstructure was immediately examined by using a HIROX KH-7700 3D-Digital microscope, and the grain size was determined by the ASTM E112-12 standard comparison method [16]. Three cross- section samples were prepared from the same UNS S-32760 SDSS rod. These sections were connected to a conductive thread and embedded in epoxy resin, with posterior roughing using a 600-pt. sandpaper and cleaned with deionised water and ethyl alcohol.

2.2 Electrochemical techniques

Electrochemical experiments were performed in a synthetic white liquor mix prepared with deionised water, 150 g/L Na(OH) and 50 g/L Na$_2$S, at a pH of 13.0, in a three-electrode cell where the working electrode was the sample under study. A saturated calomel electrode (SCE) was set as the reference electrode and a Pt grid as the counter-electrode. Electrochemical measures were done at temperatures of 25, 50, and 70°C. A GAMRY Interface
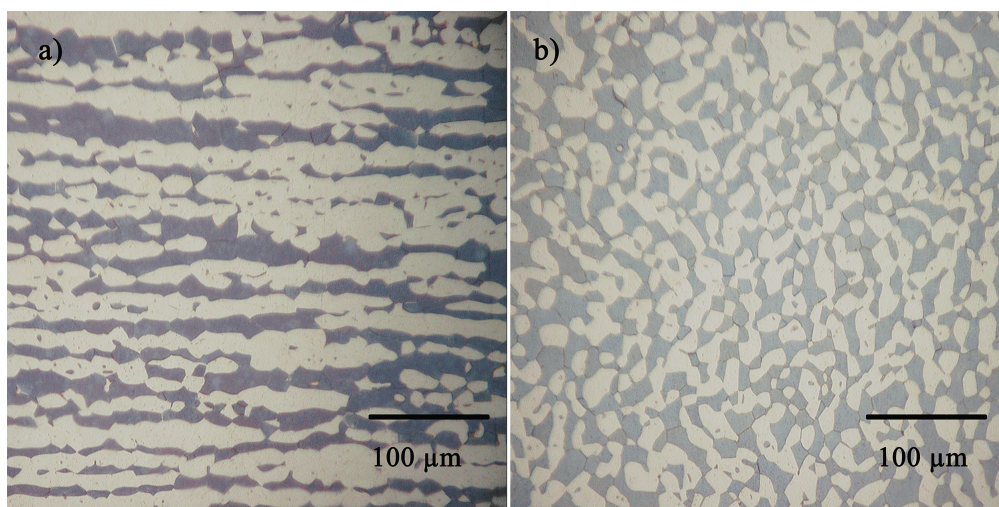
Figure 1 UNS S-32760 SDSS microstructure **a)** 700x longitudinal section **b)** 700x cross section

Table 1 Chemical composition of the UNS S-32760 SDSS (wt.%)

UNS S-32760 SDSS	Element										
	C	Si	Mn	P	S	Cr	Mo	Ni	Cu	N	W
	0.025	0.40	0.62	0.022	0.001	25.75	3.57	7.30	0.55	0.25	0.55

1000 potentiostat/galvanostat was chosen to run the CPP test. The CPP was recorded at a sweep rate of 0.167 mV/s, and the potential scan range was applied between -0.01 and 1.5 V vs SCE from the corrosion potential (Ecorr), using a complete polarisation cycle and current density limit of 5mA/cm^2, according to the ASTM G61 standard [17]. Assays were performed in triplicate.

2.3 Microstructural characterisation

Surface morphology was done using Optical Microscopy (OM), Digital Microscopy (DM), and Scanning Electron Microscopy (SEM). Observations of the cross-section micrographs of the samples were also made to determine the presence of pitting corrosion. The chemical composition of the cross-section structures was obtained by Energy Dispersive X-ray Spectroscopy (EDS).

3. Results and discussion

3.1 DM characterisation

The UNS S-32760 SDSS characterisation was achieved to identify its microstructural nature. Figure 1a presents a longitudinal image elucidating some texture, a clear indicator of the steel being mechanically deformed in such direction. On the other hand, Figure 1b shows a microstructure corresponding to a biphasic structure to which the darkest areas represent the ferrite phase (α), and the lighter regions the austenite phase (γ),

where tonality variation describes a homogeneous 50:50 distribution. In addition, a grain size number 8 was established.

Optical Emission Spectrometry (OES) using a Bruker Q8 was used to determine the chemical composition of the UNS S-32760 SDSS (Table 1), highlighting the presence of chromium, nickel, and molybdenum.

3.2 Cyclic potentiodynamic polarisation (CPP)

Figure 2 shows the UNS S-32760 CPP curves at temperatures of 25, 50, and 70°C, respectively. Curves initiate their scanning by causing the formation of a cathodic zone until corrosion potential (E_{corr}) is reached, moving to the anodic direction where the alloy exhibits an active-pseudo-passive behaviour before approaching the pitting potential (Ep) to commence the pit nucleation. This behaviour may indicate a passivating oxide film of low stability (passivity current values increase with the potential) because of competition between adsorption and dissolution processes on the alloy surface. The value for (Ep) was determined from the point where a current density value of 100μA/cm^2 was experienced during forward scanning [18].

Later, an increase in the current density is exhibited prior to hitting a 5mA/cm^2 limit value, rendering the region where the pit wells propagation is generated.
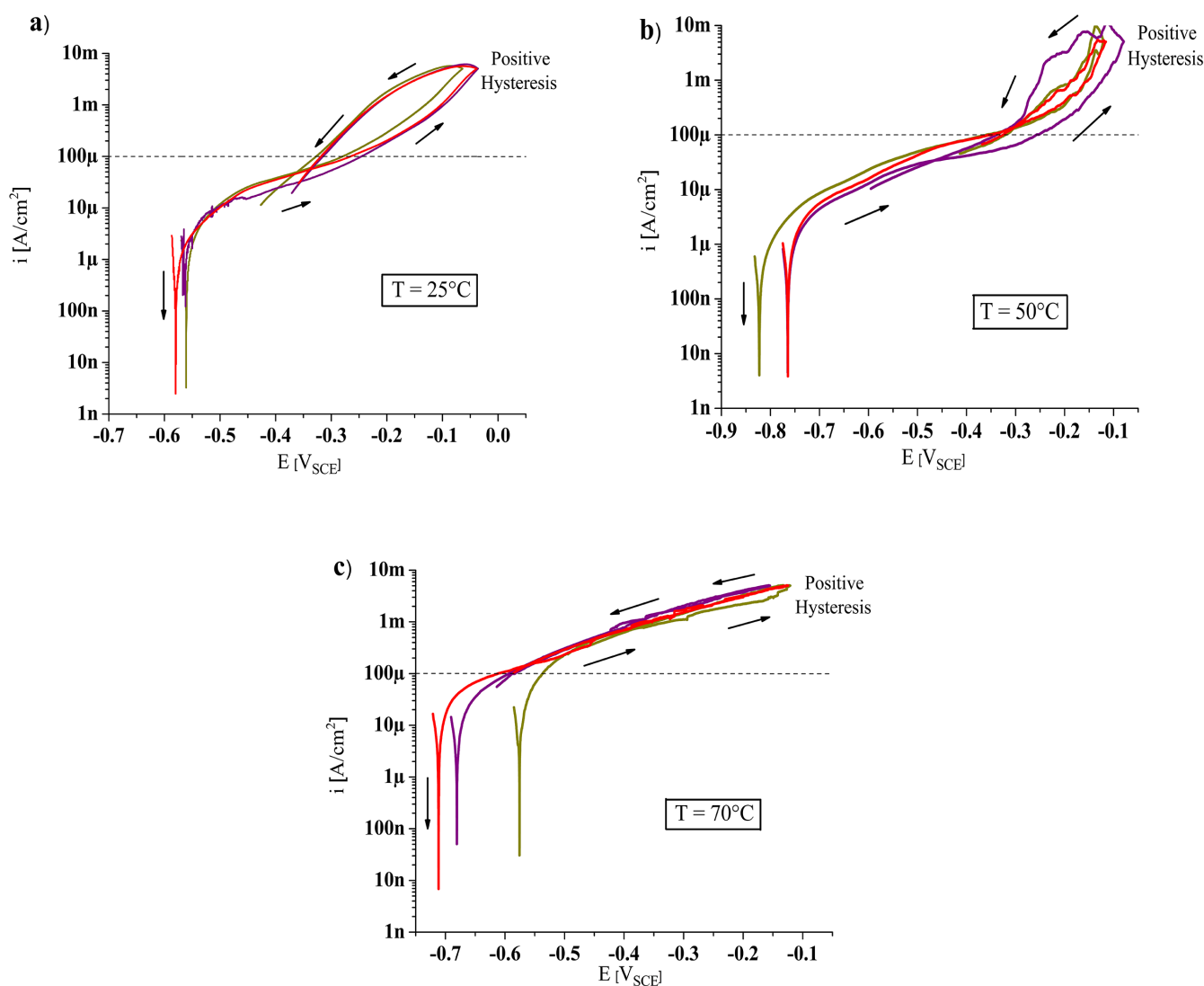
Figure 2 UNS S-32760 CPP curves in white liquor aerated aqueous solution at temperatures of **a)** 25°C **b)** 50°C **c)** 70°C

When the scanning reaches the maximum current density, a scanning starts in the cathodic direction, tracing a hysteresis loop, where the point the loop closes with the pseudo-passive area is described as the repassivation potential (Erp), potential where the passive layer is regenerated again. Figure 2 also shows that the anodic current densities of the stainless steel at reverse scanning were greater than the values for forward scanning at the same potential, resulting in a positive hysteresis for the UNS S-32760. This positive hysteresis could be understood as susceptibility to localised corrosion (pitting) [19].

Figure 2 a, b, c present the superposition of three polarisation curves that demonstrate to have the same trajectory under similar testing conditions; however, corrosion E_{corr} variations were encountered, a phenomenon attributed to the surface state and the preparation of the working electrodes, as documented by Bearvers *et al.* [20]. Samples assessed at 70°C (Figure 1C), sustained a more detailed analysis to determine the critical potentials because of the identical back and forth scanning routes. Differently, to counteract the crevice corrosion effect, specimens were isolated at the metal-resin interface to circumvent the formation of this localised corrosion type.

3.3 Pitting (Ep) and repassivation potentials (Erp)

The Ep and Erp values with their standard deviations are reported in Figure 3. Small standard deviations were obtained, implying good results reproducibility in the achieved measurements. Based on the results, Figure 3a shows that when increasing temperature, the pitting potentials tend towards more negative values, meaning
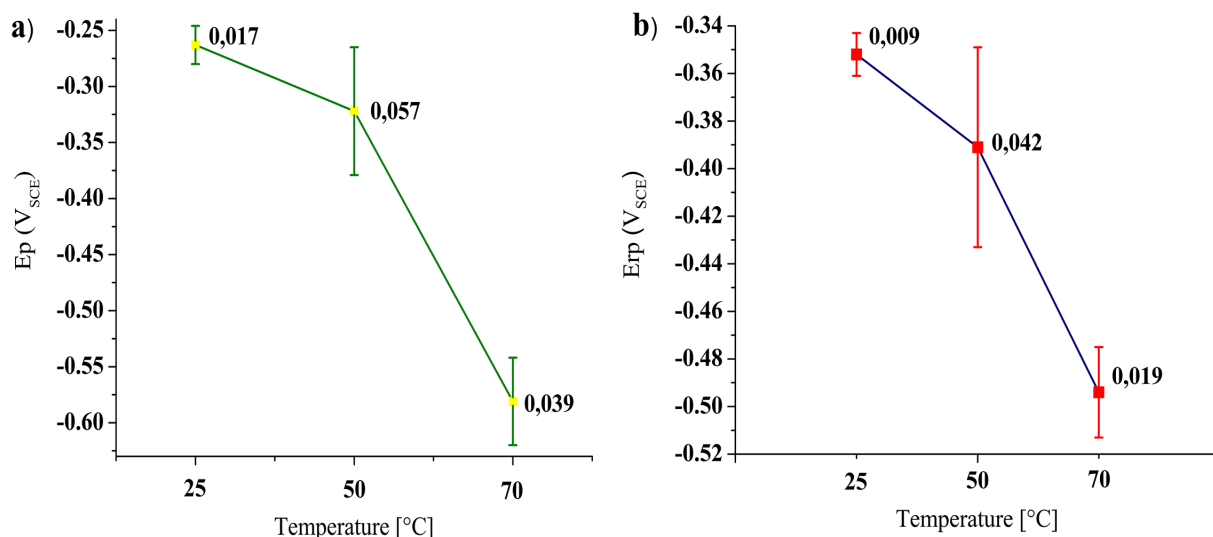
**Figure 3 a)** Alloy pitting potentials at 25, 50, and 70°C **b)** Alloy repassivation potentials at 25, 50, and 70°C

that the alloy is more susceptible to localised corrosion (pitting). Diversely, the repassivation potential (Erp) values suggest an inversely proportional variation to the temperature, as seen in Figure 3b. This behaviour is correlated to the material passive layer repair-ability. Moreover, an increase in temperature makes the Ep and Erp values set apart, causing the reduction of the pseudo-passivity zone.

3.4 Temperature effect

Figure 4 shows the behaviour of the alloy in respect of the temperature. The sample exposed to 70°C demonstrates the most active pitting potential; therefore, the UNS S-32760 SDSS is more likely to pitting corrosion at high temperatures. At 25°C pitting corrosion is evidenced, in response to the medium aggressiveness. At a temperature of 50°C, there is a short distance between the Erp and Ep, showing little growth pit wells since the protective material film has surrendered stability. At 70°C, there is a remarkable difference between the Ep and Erp, and at this temperature, the higher pitting wells quantity and growth are attained. In addition, the Erp value is nearer to the Ecorr; hence the nucleation and pitting progress is more critical. Within the pits, the thiosulphate ion ($S_2O_3^{-2}$) is more stable, a phenomenon that accelerates the corrosion process and impedes the alloy repassivation, as reported by Laitinen *et al.* [21].

3.5 Microstructural analysis

To observe and identify the morphology of the material, OM and SEM techniques were applied to perform the microscopic analysis of the samples exposed to the aggressive medium at 70°C. Figure 5 shows the
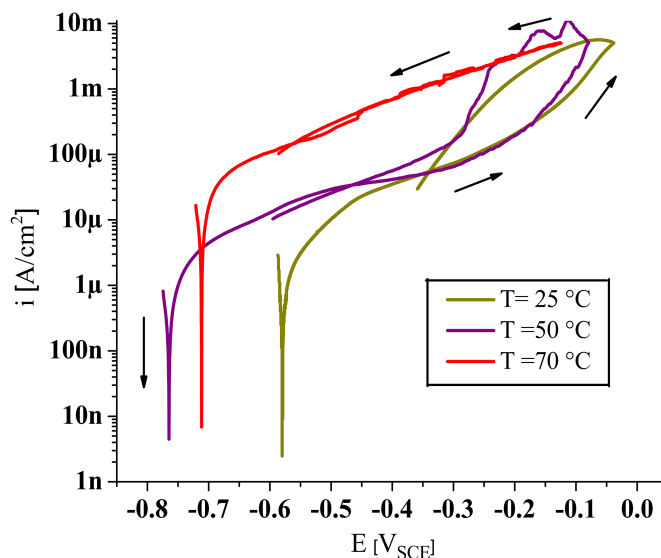

Figure 4 UNS S-32760 CPP curves in white liquor aerated aqueous solution at temperatures of 25, 50 and 70°C

semi-protective layer damage on the metal, since a surface with light and dark noticeable discontinuity areas is appreciated because of the lack of presence of a stable film; additionally, small pits are perceived with a not fully circular morphology. These pits have dimensions less than 20μm and are described in Figure 5d as the darkest areas.

Figure 6 shows the 3D digital reconstruction of a single pit on the UNS S-32760 SDSS after CPP. This pit was formed in a white liquor solution at 70°C. Overall, the pits on the UNS S-32760 SDSS were open and hemispherical. The pit depth is approximately 58.16 μm.
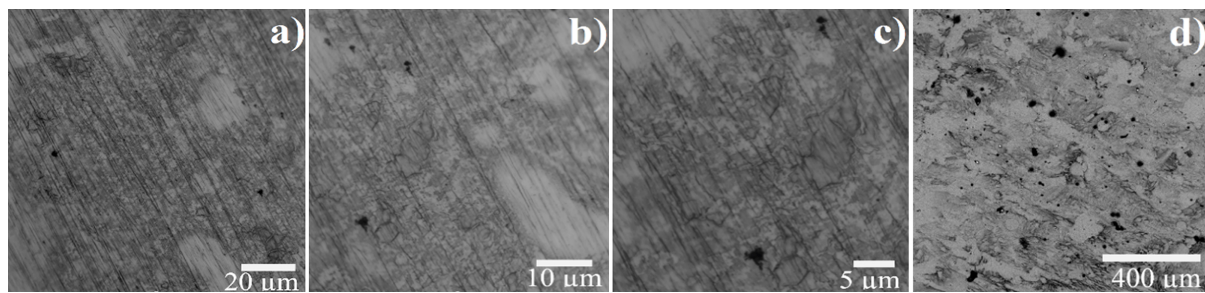
Figure 5 Micrograph of the UNS S-32760 SDSS exposed to the CPP technique in white liquor aerated aqueous solution at 70°C. Sample observed with the Optical Microscope **a)** 500x, **b)** 1000x and **c)** 1500x. Sample observed with the Scanning Electron Microscope **d)** 200x
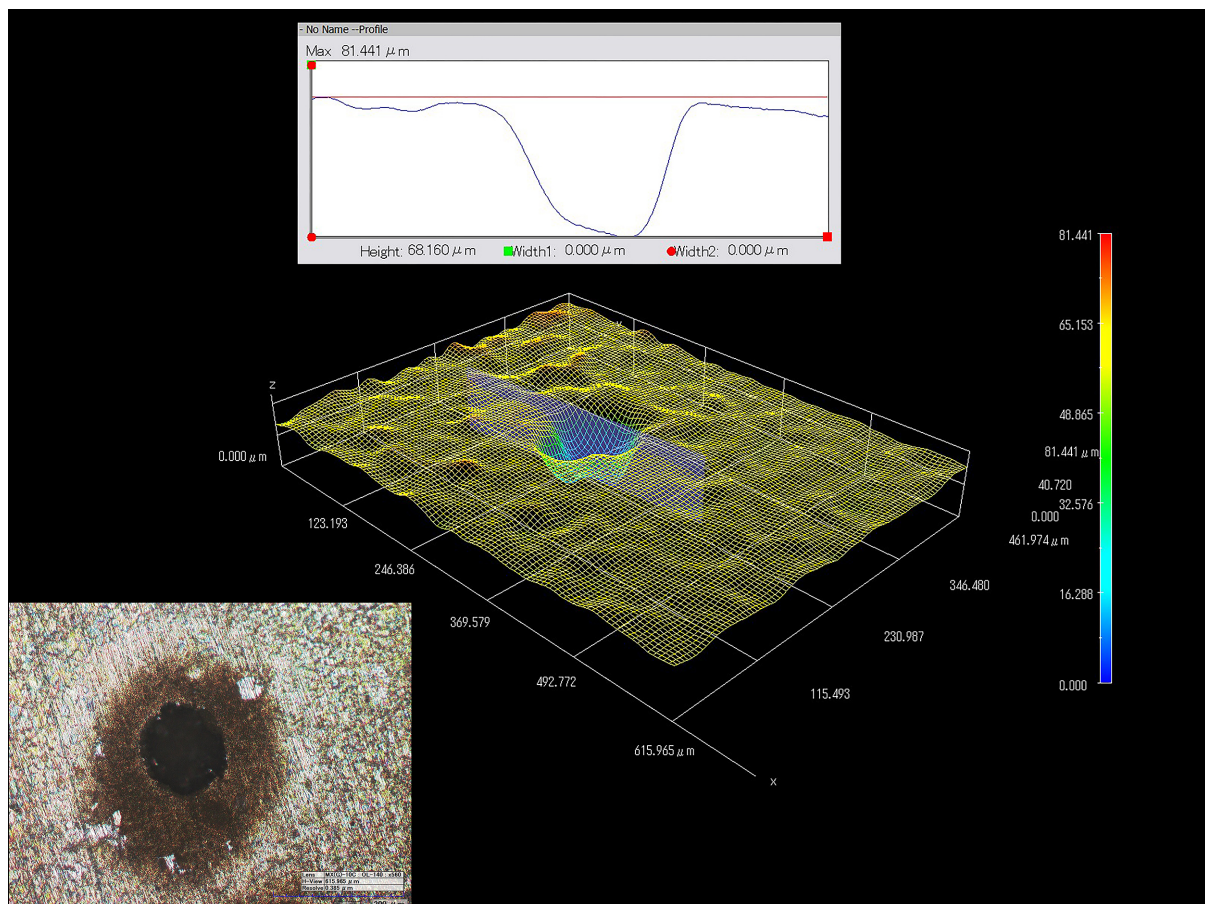

Figure 6 3D digital reconstruction of a single pit on the UNS S-32760 SDSS exposed to the CPP technique in white liquor aerated aqueous solution at 70°C

Furthermore, SEM-EDS measurements were taken on some sample surface spots to acquire a semi-quantitative analysis and detect the existence of elements that promote the formation of the protective and pitting layer. Figure 7 evinces the presence of chromium, nickel, and oxygen, elements required for the formation of chromium and nickel oxides, both responsible for the passive layer formation; however, the presence of sulphur ions that produce the degradation and instability of the protective layer is noticed likewise.

Measurements were registered in other areas corresponding to the etched surface, as shown in Figure 8. Cr and Ni elements are seen, yet little presence of oxygen was detected, indicating that the protective layer of the material is weakened, explaining the non-homogeneous characteristic throughout the metal surface.

Element	At %
O	32.27
S	0.16
Cr	11.35
Ni	2.47
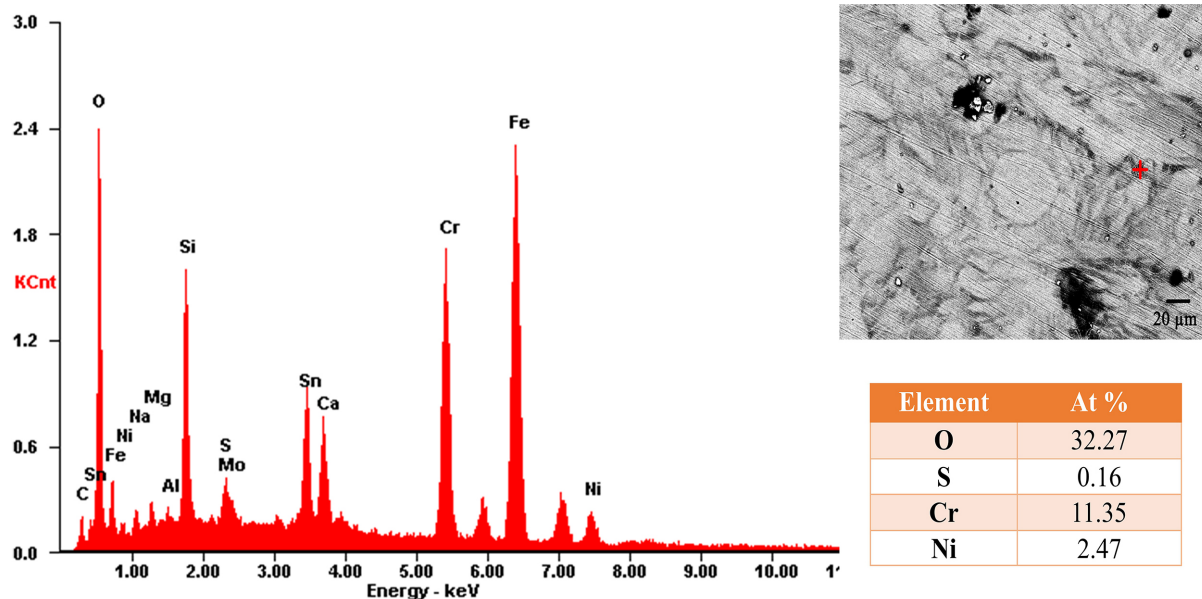
Figure 7 EDS analysis in the UNS S-32760 dark zone of the layer

| Element	At %
Fe	55.65
O	1.29
Cr	27.98
Ni	5.65
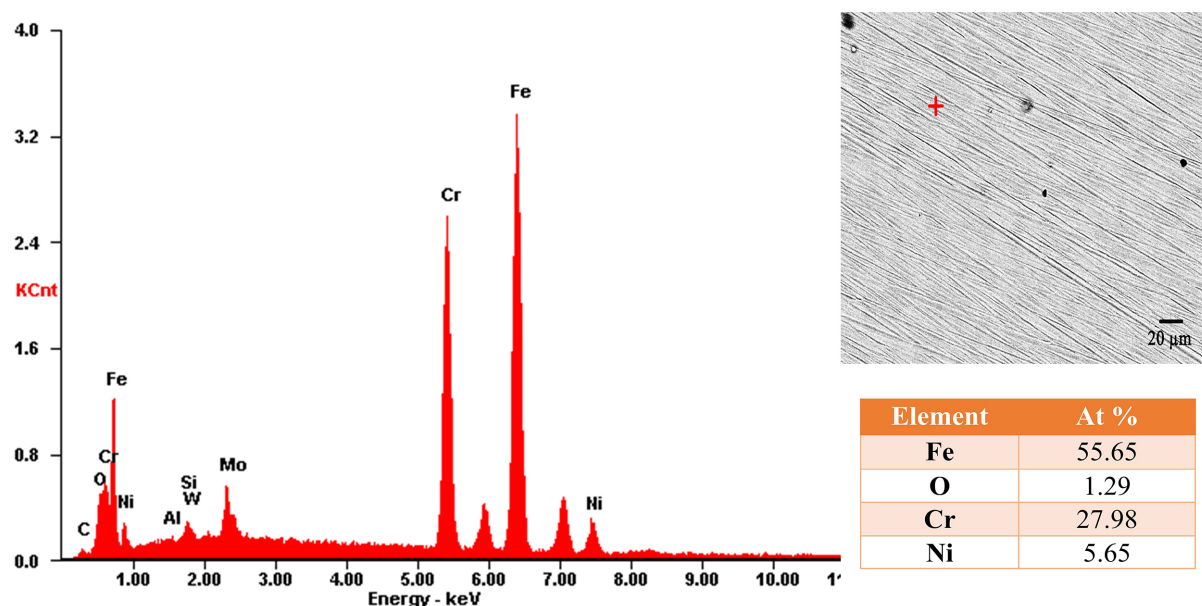
Figure 8 EDS analysis in the UNS S-32760 light zone of the layer

Figure 9 shows the EDS spectrum within a pit, highlighting substantial oxygen contents that establish inclusions of (Mg, Al) oxides being the preferable zones towards the formation of pitting in the alloy, as reported by H. Feng [4] in his research work; besides, there is validation that in these sites prevail a greater concentration of sulphide ions that generate the pitting in-growth and development.

3.6 Corrosion mechanism

Compounds like sodium hydroxide (NaOH) and sodium sulphide (Na$_2$S) are present in the Kraft pulping white liquor. Thus, the active species are hydrogen sulphide (HS$^-$) and hydroxide (OH$^-$) ions [13]. In solution, Na$_2$S is dissolved into hydroxide and hydrogen sulphide ions according to Equation 1:

$$S^{2-} + H_2O \leftrightarrow OH^- + HS^- \qquad (1)$$
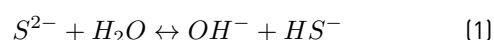
The HS$^-$ can be further hydrolysed as observed in reaction (2):

$$HS^- + H_2O \leftrightarrow H_2S_{(aq)} + OH^- \qquad (2)$$
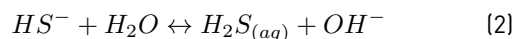
The sulphide could exist as HS$^-$, S^{2-}, and dissolved H$_2$S in aqueous solutions. However, at high pH units, the sulphide
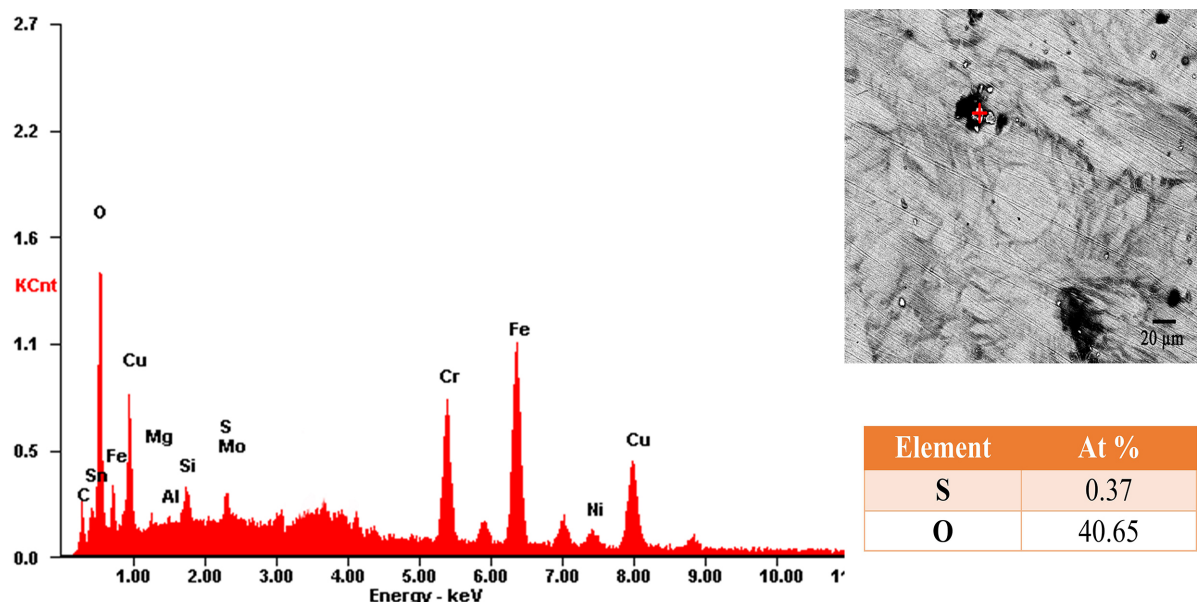
is present as H_2S and HS^-. The relative amounts of either compound depend on the concentration of hydroxide ions and the numerical value of the equilibrium constants, since the three sulphide compounds are in equilibrium with each other. The equilibrium constants depend on the temperature and the ionic strength.
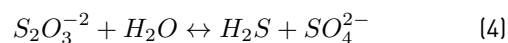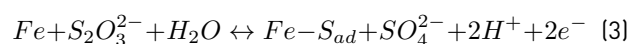
Industrial white liquor also contains other compounds in smaller amounts. Sulphate (SO_4^{2-}), carbonate (CO_3^{2-}), sulphite (SO_3^{2-}) and thiosulphate ($S_2O_3^{2-}$) ions are present in concentrations of 0.04, 0.3, 0.03 and 0.007 [mole/l], respectively. While the sulphate stems from incomplete reduction of sulphide in the recovery furnace, the carbonate originates from incomplete conversion of carbonate to hydroxide in the causticizing, and the thiosulphate is obtained from the HS^- oxidised by air [22].

The proposed pitting corrosion mechanism in the UNS S-32760 SDSS exposed to a white liquor synthetic solution can be evaluated considering parameters such as the concentration and diffusion of species.

Concentration mechanism

The passivation depends mainly on hydrogen sulphide (HS^-) and hydroxide (OH^-) ions concentration in the system. These ions are responsible for precluding or strengthening the passive layer [21, 23, 24]. Sulphur was found in the pits, as evidenced by the EDS results (Figure 9). The formation of the sulphur layer on the stainless steel dissolving surface, leads to a catalytic process and reduces the activation energy for metal dissolution [21, 24, 25]. Sulphides cause retardation of the passive layer formation

in the environments containing sulphur species and could promote pitting corrosion in potential ranges between 0.15V and 0.35V [25]. Other sulphur ions (SO_4^{2-}, SO_3^{2-}, $S_2O_3^{2-}$) may adhere in the oxide inclusions and help initiate pits nucleation. The following reactions (Equation 3 and 4) represent the iron dissolution and H_2S formation as presented by Naghizadeh *et al.* [25].

$$Fe + S_2O_3^{2-} + H_2O \leftrightarrow Fe-S_{ad} + SO_4^{2-} + 2H^+ + 2e^- \quad (3)$$

$$S_2O_3^{-2} + H_2O \leftrightarrow H_2S + SO_4^{2-} \quad (4)$$

If $S_2O_3^{2-}$ ion is present in solution, the formation of sulphur due to the reduction of $S_2O_3^{2-}$ occurred, which is afterwards reduced to H_2S. Metal corrosion rates could be increased by the presence of the H_2S adsorbed on the metal surface. Consequently, it is essential to note that, although the thiosulphate ion ($S_2O_3^{2-}$) impedes the formation of a passive layer, it does not promote pitting growth. Likewise, the presence of sulphate ions (SO_4^{-2}) and inclusions (globular oxides, sulphurs) are necessary to guarantee the beginning of localised corrosion in this class of alloys [8, 21, 23]. Particularly, sulphate ions are the sulphur stable form in white liquor, and these ions increase conductivity and corrosion rates [26].

On the other hand, the molybdenum concentration in steel must be considered since the presence of this element decreases the activating effect of sulphur species [20]. It was further shown that a higher thiosulphate concentration was required for pit activation with an increase in the molybdenum content in stainless steel [27]. Moreover, when molybdenum is present in stainless
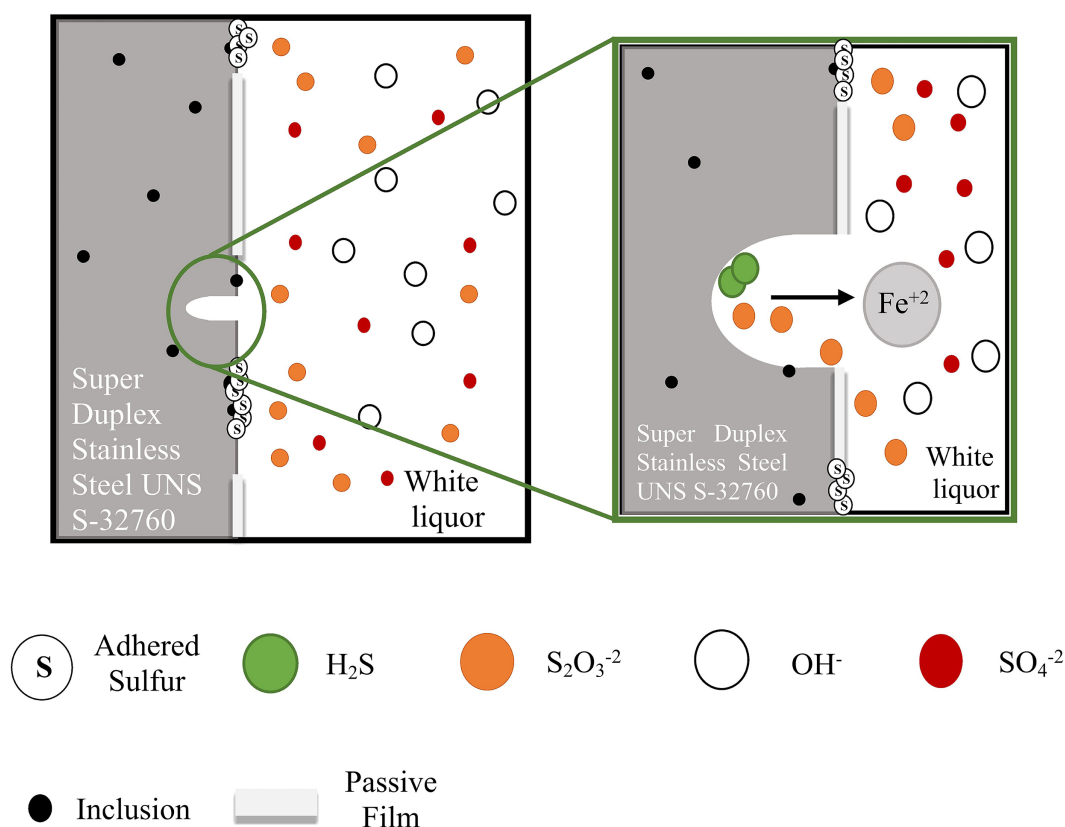
Figure 10 Representative diagram of the corrosion mechanism in a UNS S-32760 super duplex stainless steel in a white liquor synthetic solution

steels or nickel alloys, the sulphur is unstable as S0 and reduced to aqueous H_2S [25].

Diffusion mechanism

When thiosulphate is present in the white liquor solution, it can migrate into the growing pits. Thiosulphate ($S_2O_3^{2-}$) ions into the pits are reduced to form H2S, increasing corrosion kinetics, and contributing to the iron dissolution and pitting growth. However, when no thiosulphate is present in the white liquor or the concentration is negligible, sulphide inclusions (MnS) are responsible for pits nucleation. Equally, the presence of nickel and copper in the UNS S-32760 SDSS can be precursors in forming stable sulphides such as (NiS) and (Cu2S), with potentials above -500mV, as mentioned by Laitinen *et al.* [21].

Figure 10 shows a representative corrosion process model in a UNS S-32760 SDSS in a white liquor synthetic solution. The different ions and compounds (S, OH⁻, $S_2O_3^{2-}$ SO_4^{2-}, H_2S) are present in the solution. Sulphur is suggested to block the adsorption sites of hydroxyl ions, which are the precursors in the formation of the passive layer. The accumulation of sulphur ions on the inclusion surface is proposed. Pits' formation and growing are

mainly attributed to the reduction of thiosulphate ions forming H_2S, which increases the formation of localised corrosion (pitting).

4. Conclusions

- Cyclic potentiodynamic polarisation of the UNS S32760 super duplex stainless steel showed positive hysteresis and higher Erp than Ecorr values under test conditions, indicating that this material is susceptible to pitting corrosion.

- The increase of temperature significantly reduced the pitting corrosion resistance of the alloy in white liquor solution since the Ep and Erp values became more active.

- The presence of a non-uniform layer on the alloy surface was confirmed through the EDS carried out on the sample exposed to 70°C, establishing sulphur atomic percentage amounts within the pits, explaining its participation in the corrosion process or mechanism. In addition, high oxygen concentrations are registered in the pits, which may indicate that the pits' nucleation takes place in the inclusions of oxides.

- The formation and growth of pitting could be attributed to the reduction of thiosulphate ions that form H2S, which increases the localised corrosion.

- The optical and scanning electron microscopy results showed the morphology of damage, exhibiting localised corrosion and corroborating the existence of a relationship between temperature and pitting corrosion kinetics of the UNS S-32760 super duplex steel when exposed to the white liquor solution.

5. Declaration of competing interest

We declare that we have no significant competing interests, including financial or non-financial, professional, or personal interests interfering with the full and objective presentation of the work described in this manuscript.

6. Acknowledgments

References

[1] M. M. Ramírez, "La reproducción de la imagen y su impacto en la construcción de nuevas realidades: historia del papel y de la imprenta en el continente americano," *Ámbitos*, no. 13-14, Jan. 17, 2005. [Online]. Available: http://dx.doi.org/10.12795/Ambitos.2005.i13-14.15

[2] K. Teschke and P. Demers, "Industria del papel y de la pasta de papel-sectores basados en recursos biológicos," in *Enciclopedia de salud y seguridad en el trabajo III*, B. Chantal Dufresne, Ed. Madrid: Ministerio de Trabajo y Asuntos Sociales, Subdirección General de Publicaciones, 2001, pp. 71.1–72.21. [Online]. Available: https://prevencionar.com/2020/02/17/enciclopedia-de-salud-y-seguridad-en-el-trabajo-volumen-iii/

[3] D. C. Crowe, "Stress corrosion cracking of carbon steel in kraft digester liquors," in *Proceedings of the 6th International Symposium on Corrosion in the Pulp & Paper Industry*, Helsinki, 1989, pp. 35–47. [Online]. Available: https://smartech.gatech.edu/bitstream/handle/1853/2505/tps-339.pdf

[4] H. Feng, H. Li, and *et al.*, "Corrosion behavior of super duplex stainless steel s32750 in white liquor," *Internation Journal Electrochemical Science*, no. 10, 2015. [Online]. Available: t.ly/JBxf

[5] A. Bhattacharya and P. Singh, "Electrochemical behaviour of duplex stainless steels in caustic environment," *Corrosion Science*, no. 1, Jan. 2011. [Online]. Available: https://doi.org/10.1016/j.corsci.2010.09.024

[6] A. Sharma, Sulaxna, and A. K. Singh, "Corrosion investigations due to increased sulfidity in digester house of paper mill," *Journal of Materials and Environmental Science*, vol. 3, no. 6, Jul. 24, 2012. [Online]. Available: https://www.jmaterenvironsci.com/Document/vol3/vol3_N6/102-JMES-246-2012-Sharma.pdf

[7] A. Wensley, "Corrosion of carbon and stainless steels in kraft digesters," Presented at NACE Corrosion 2000 Conference, Orlando, FL, 2000. [Online]. Available: https://onepetro.org/NACECORR/proceedings-abstract/CORR00/All-CORR00/NACE-00589/111599

[8] M. D. López, "Resistencia a la corrosión de aceros inoxidables de última generación en medios que contienen cloruros y mezclas cloruro-fluoruro," PhD. thesis, Dept. de Ciencia de los Materiales e Ingeniería Metalúrgica, Universidad Complutense de Madrid, Madrid, Spain, 2003. [Online]. Available: https://eprints.ucm.es/id/eprint/3553/

[9] A. Wensley, "Corrosion in alkaline pulping liquors," Presented at NACE Corrosion 2004 Conference, New Orleans, LA, 2004. [Online]. Available: https://onepetro.org/NACECORR/proceedings-abstract/CORR04/All-CORR04/NACE-04248/115662

[10] D. Singbeil and A. Garner, "Electrochemical and stress corrosion cracking behavior of digester steels in kraft white liquors," *Corrosion: The Journal of Science and Engineering*, vol. 41, no. 11, Nov. 01, 1981. [Online]. Available: https://doi.org/10.5006/1.3582997

[11] R. Davalos, J. V. de Wetering, B. Krawczyk, and D. L. Engelberg, "Corrosion behaviour of type 316l stainless steel in hot caustic aqueous environments," *Metals and Materials Internaional*, no. 26, Oct. 20, 2019. [Online]. Available: https://doi.org/10.1007/s12540-019-00403-2

[12] A. Wensley and P. Champagne, "Effect of sulfidity on the corrosivity of white, green, and black liquors," Presented at the Corrosion 99 Conference, San Antonio, TX, 1999. [Online]. Available: https://onepetro.org/NACECORR/proceedings-abstract/CORR99/All-CORR99/NACE-99281/128306

[13] I. Betova, M. Bojinov, O. Hyökyvirta, and T. Saario, "Effect of sulphide on the corrosion behaviour of aisi 316l stainless steel and its constituent elements in simulated kraft digester conditions," *Corrosion Science*, vol. 52, no. 4, Apr. 2010. [Online]. Available: https://doi.org/10.1016/j.corsci.2009.12.034

[14] C. M. Méndez and E. R. Ruiz, "Evaluación de aceros inoxidables duplex para la construcción de un digestor," *Revista Ciencia y Tecnología*, no. 16, Dec. 20, 2011. [Online]. Available: https://www.fceqyn.unam.edu.ar/recyt/index.php/recyt/article/view/486

[15] L. Esteves, M. Cardoso, and V. de Freitas Cunha Lins, "Corrosion behavior of duplex and lean duplex stainless steels in pulp mill," *Materials Research*, vol. 21, no. 1, Dec. 18, 2017. [Online]. Available: https://doi.org/10.1590/1980-5373-mr-2017-0148

[16] *ASTM E112-12, Standard Test Methods for Determining Average Grain Size*, ASTM International, 2012. [Online]. Available: https://doi.org/10.1520/E0112-12

[17] *ASTM G61-86, Standard Test Method for Conducting Cyclic Potentiodynamic Polarization Measurements for Localized Corrosion Susceptibility of Iron, Nickel, or Cobalt-based Alloys*, ASTM International, 2018. [Online]. Available: https://doi.org/10.1520/G0061-86R18

[18] *ASTM G150-18, Standard Test Method for Electrochemical Critical Pitting Temperature Testing of Stainless Steels and Related Alloys*, ASTM International, 2018. [Online]. Available: https://doi.org/10.1520/G0061-86R18

[19] A. Pasha, H. M. Ghasemi, and J. Neshati, "Study of the pitting corrosion of superduplex stainless steel and x-65 carbon steel during erosion–corrosion by cyclic polarisation technique," *The International Journal of Corrosion Processes and Corrosion Control*, vol. 51, no. 6, May. 20, 2016. [Online]. Available: https://doi.org/10.1080/1478422X.2016.1141546

[20] J. A. Beavers, N. G. Thompson, and C. L. Durr, "Unique interpretations of potentiodynamic polarization technique," Presented at the Corrosion 98 Conference, San Diego, CA, 1998. [Online]. Available: https://onepetro.org/NACECORR/proceedings-abstract/CORR98/All-CORR98/NACE-98300/127701

[21] T. Laitinen, "Thiosulfate pitting corrosion of stainless steels in paper machine environment," PhD. thesis, VTT Manufacturing Technology, Helsinky University of Technology, Espoo, FI, 1999. [Online]. Available: https://www.vttresearch.com/sites/default/files/pdf/publications/1999/P399.pdf

[22] "Pulping chemistry and technology," in *Pulp and Paper Chemistry and Technology*, M. E.k, G. Gellerstedt, and G. Henriksson, Eds. Stockholm, SWE: Walter de Gruyter, 2009, vol. 2.

[23] M. M. Benyahya, "Corrosion behaviour of austenitic steels in basic thiosulfate gold leaching environments," PhD. thesis, Materials Engineering, The University of British Columbia, Vancouver, CA, 2013. [Online]. Available: https://open.library.ubc.ca/cIRcle/collections/ubctheses/24/items/1.0073673

[24] S. M. A. E. Haleem and E. E. A. E. Aal, "Electrochemical behaviour of iron in alkaline sulphide solutions," *The International Journal of Corrosion Processes and Corrosion Control*, vol. 43, no. 2, Nov. 27, 2013. [Online]. Available: https://doi.org/10.1179/174327807X234769

[25] M. Naghizadeh, D. Nakhaie, M. Zakeri, and M. H. Moayed, "Effect of thiosulfate on pitting corrosion of 316ss: I. critical pitting temperature and pit chemistry," *Journal of The Electrochemical Society*, vol. 162, no. 1, Nov. 26, 2014. [Online]. Available: https://doi.org/10.1149/2.0861501jes

[26] "Asm handbook volume 13c: Corrosion: Environments and industries," 2006. [Online]. Available: https://www.asminternational.org/search/-/journal_content/56/10192/05145G/PUBLICATION

[27] L. Choudhary, D. D. Macdonald, and A. Alfantazi, "Role of thiosulfate in the corrosion of steels: A review," *Corrosion: The Journal of Science & Engineering*, vol. 71, no. 9, Jun. 01, 2015. [Online]. Available: https://doi.org/10.5006/1709